Editors' Suggestion

Prevailing Charge Order in Overdoped $La_{2-x}Sr_xCuO_4$ beyond the Superconducting Dome

Qizhi Li,[1,*] Hsiao-Yu Huang,[2,*] Tianshuang Ren,[3,*] Eugen Weschke,[4] Lele Ju,[3] Changwei Zou,[1] Shilong Zhang,[1] Qingzheng Qiu,[1] Jiarui Liu,[5] Shuhan Ding,[5] Amol Singh,[2] Oleksandr Prokhnenko,[4] Di-Jing Huang,[2] Ilya Esterlis,[6] Yao Wang,[5,7] Yanwu Xie,[3] and Yingying Peng[1,8,†]

[1]*International Center for Quantum Materials, School of Physics, Peking University, Beijing 100871, China*
[2]*National Synchrotron Radiation Research Center, Hsinchu 30076, Taiwan*
[3]*Interdisciplinary Center for Quantum Information, State Key Laboratory of Modern Optical Instrumentation, and Zhejiang Province Key Laboratory of Quantum Technology and Device, Department of Physics, Zhejiang University, Hangzhou 310027, China*
[4]*Helmholtz-Zentrum Berlin für Materialien und Energie, Berlin 14109, Germany*
[5]*Department of Physics and Astronomy, Clemson University, Clemson, South Carolina 29631, USA*
[6]*Department of Physics, Harvard University, Cambridge, Massachusetts 02138, USA*
[7]*Department of Chemistry, Emory University, Atlanta, Georgia 30322, USA*
[8]*Collaborative Innovation Center of Quantum Matter, Beijing 100871, China*

(Received 30 September 2022; revised 3 April 2023; accepted 24 August 2023; published 14 September 2023)

The extremely overdoped cuprates are generally considered to be Fermi liquid metals without exotic orders, whereas the underdoped cuprates harbor intertwined states. Contrary to this conventional wisdom, using Cu L_3-edge and O K-edge resonant x-ray scattering, we reveal a charge order (CO) correlation in overdoped $La_{2-x}Sr_xCuO_4$ ($0.35 \leq x \leq 0.6$) beyond the superconducting dome. This CO has a periodicity of ~6 lattice units with correlation lengths of ~20 lattice units. It shows similar in-plane momentum and polarization dependence and dispersive excitations as the CO of underdoped cuprates, but its maximum intensity differs along the c direction and persists up to 300 K. This CO correlation cannot be explained by the Fermi surface instability and its origin remains to be understood. Our results suggest that CO is prevailing in the overdoped metallic regime and requires a reassessment of the picture of overdoped cuprates as weakly correlated Fermi liquids.

DOI: 10.1103/PhysRevLett.131.116002

High-temperature superconductivity (SC) is a great surprise in quantum materials and its mechanism remains a puzzle. In the past 37 years, studies on cuprate superconductors primarily have been focused on the underdoped and optimally doped regions—close to the Mott-insulating state of the phase diagram [1,2]. It has been a long-standing challenge to understand how the versatile phenomena exhibited in these materials, such as the pseudogap (PG) and strange metal states, together with a plethora of exotic electronic orders, coexist and compete with superconductivity [2]. On the contrary, the overdoped region is generally considered to be a conventional Fermi liquid (FL) and less affected by the doped-Mott-insulator scenario [1]. However, the doping and temperature dependencies of the superfluid density are incompatible with the standard BCS description, suggesting phase fluctuations in the overdoped region [3]. These fluctuations are characterized by photoemission as preformed Cooper pairs well above T_c [4] and magnetic fluctuations persistent in the extremely overdoped regime [5]. Moreover, ferromagnetism has been discovered in overdoped $(Bi,Pb)_2Sr_2CuO_{6+\delta}$ (Bi2201) [6] and beyond the superconducting dome in $La_{2-x}Sr_xCuO_4$ [7]. These discoveries suggested that strong electronic correlations remain present in the overdoped cuprates.

Charge orders are ubiquitous in underdoped cuprates [2,8–16] and have enigmatic interactions with SC [10,11] and PG [12]; however, there is still no consensus on the underlying mechanism with ongoing debates including the real-space electronic correlation scenario [14,16] versus the momentum-space instability scenario [12]. The latter has been challenged by one resonant x-ray scattering study that observed charge order in heavily overdoped Bi2201 whose Fermi surface lacks the nesting features [17]. The distribution and doping evolution of charge order (CO) provides a route by which to test how close the overdoped systems are to a FL, and also quantify the underlying fluctuations. Therefore, it is of great importance to assess the universality of charge ordering in overdoped cuprates, which will not only have the potential to elucidate the mechanism of CO instabilities but also provide a valuable perspective to understand the complex phase diagram coming from the overdoped regime.

In this Letter, we report the existence of charge order correlation in heavily overdoped $La_{1.55}Sr_{0.45}CuO_4$ thin

 © 2023 American Physical Society

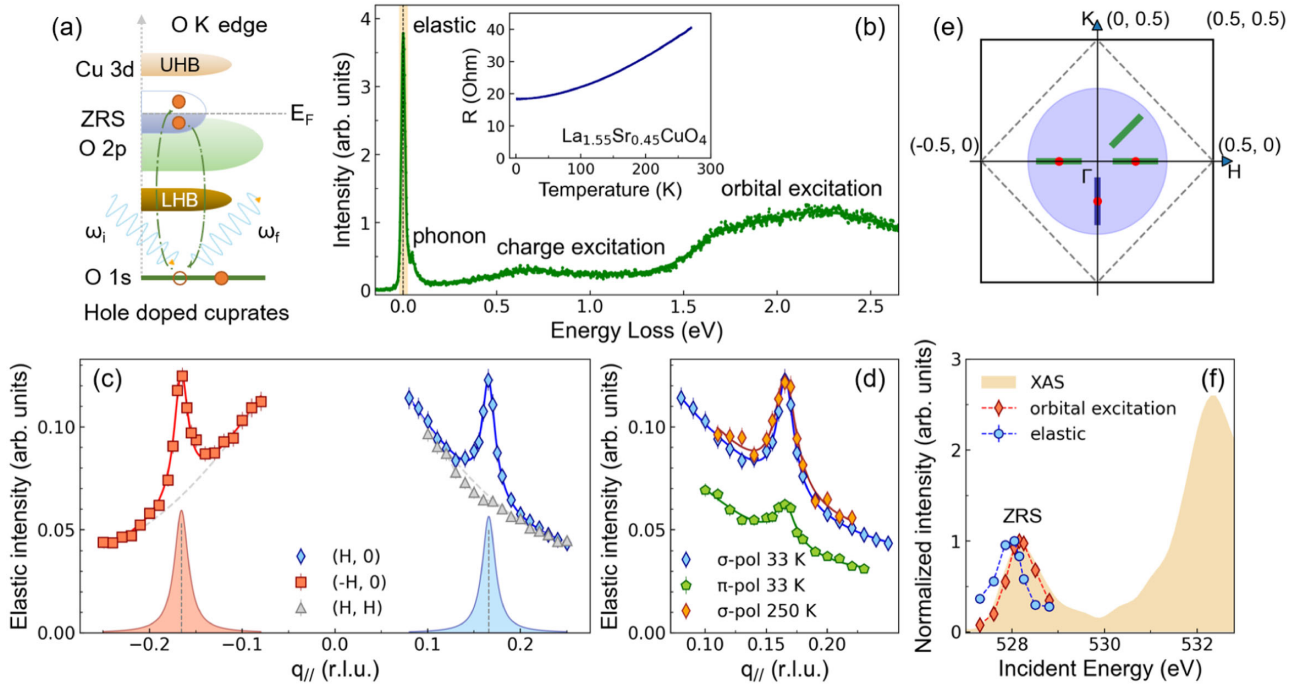

FIG. 1. Observation of charge order correlation by RIXS in overdoped metallic $La_{2-x}Sr_xCuO_4$ ($x = 0.45$). The UHB and LHB refer to upper Hubbard band and lower Hubbard band, respectively. (a) Schematic plot of RIXS process at O K edge. (b) A typical RIXS spectrum at $\mathbf{q}_{||} = (0.12, 0)$, displaying the elastic peak, phonon, charge, and orbital excitations. Inset: resistance curve displaying the metallic nature of the sample. (c) Integrated intensity of elastic peaks for positive and negative $(H, 0)$ and (H, H) directions, using σ polarization. Red and blue curves are Lorentzian peak fits to the data with a polynomial background (gray dashed lines). (d) Polarization measurements with σ- and π-polarized light, collected at 33 and 250 K. (e) Reciprocal-space image. The blue shaded region is the accessible momentum-transfer range of O K edge. The green and blue lines indicate the momentum cuts, and red dots indicate the observed CO peaks. (f) XAS spectra near the ZRS absorption peak with σ polarization at normal incidence. Incident energy dependence of the integrated intensity of elastic peak and orbital excitation, normalized to the value at the ZRS peak.

films beyond the superconducting dome (sample growth and characterizations are described in the Supplemental Material, Sec. 1 [18]. The energy resolution of oxygen K-edge resonant inelastic x-ray scattering (RIXS) is ~30 meV at 41 A Taiwan photon source. Figure 1(a) displays the schematic electronic structure of hole-doped cuprates and illustrates the resonant absorption as well as the scattering processes at oxygen K edge ($1s \rightarrow 2p$). The Zhang-Rice singlet (ZRS), originating from the hybridization between oxygen ligands and Cu $3d_{x^2-y^2}$ orbitals, manifests as a preedge peak in the x-ray absorption spectra (XAS) [30]. Figure 1(b) exemplifies the observed excitations in a metallic $La_{2-x}Sr_xCuO_4$ (LSCO) with $x = 0.45$ [resistivity shown in the inset of Fig. 1(b)], including the elastic peak, phonons (~0.05 eV), charge excitations (~0.6 eV) [19], and oxygen orbital excitations (>1.5 eV). Given the relevance to CO [10,31,32], we focus on the elastic peak and low-energy phonons below.

The elastic scattering displays a prominent peak at the planar wave vector $q_{||} = (0.165, 0)$. The FWHM of the peak is $\sim 0.017 \pm 0.002$ reciprocal lattice units (r.l.u.) with a correlation length of ~70.8 Å. This feature is symmetric along both $(H, 0)$ and $(-H, 0)$ directions but absent along diagonal (H, H) directions [Fig. 1(c)] (see RIXS map in Supplemental Material, Fig. S5) [18]. Its intensity is more pronounced for σ polarization than for π polarization at positive $\mathbf{q}_{||}$ [Fig. 1(d)], consistent with a charge scattering rather than spin scattering in the $3d^9_{x^2-y^2}$ ground state symmetry of cuprates [10]; the peak is nearly unchanged at temperatures as high as 250 K [Fig. 1(d)], as demonstrated by the temperature-dependent width and integrated intensity of the CO peak (see Supplemental Material, Fig. S5) [18]. This behavior closely resembles that of the CO observed in overdoped Bi2201 [17]. Figure 1(f) shows the intensity of the integrated elastic peak and orbital excitation as a function of incident photon energy compared with XAS. The orbital excitation follows the XAS spectrum, while the integrated elastic peak exhibits a clear resonance slightly below the absorption maximum, in analogy to the behavior of COs in underdoped cuprates [9,32,33]. The spectral weight of the ZRS peak is widely regarded as a measure of the hole density [9], so the resonance profile demonstrates a significant modulation of the doped-hole density. We have further revealed that lattice is weakly involved with this peak from nonresonant x-ray scattering measurements, which bears similarities to the

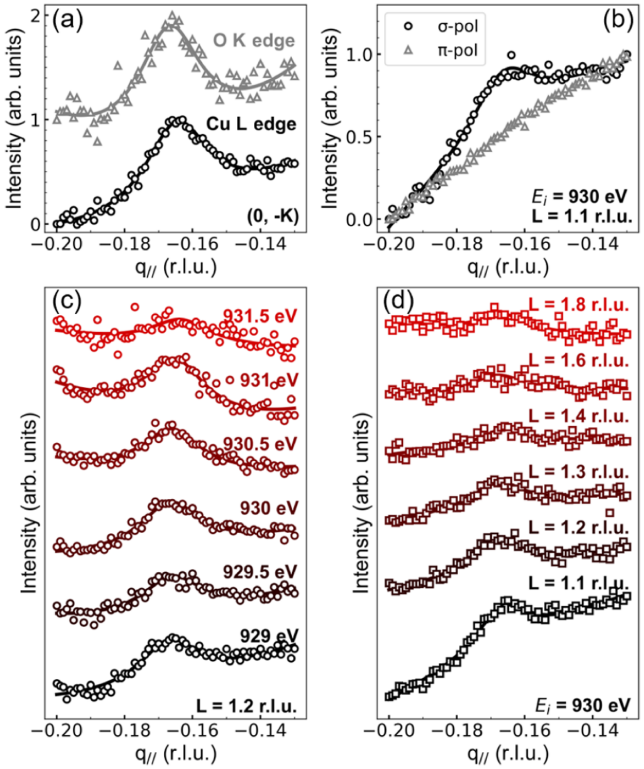

FIG. 2. Cu L_3 edge and O K edge REIXS studies of charge order correlation in $La_{1.55}Sr_{0.45}CuO_4$. (a) Observation of CO correlation along $(0, -K)$ direction at both Cu L_3 edge and O K edge, offset is applied for clarity. (b) Polarization dependence of the CO peak, collected at 930 eV and $L = 1.1$ r.l.u. (c) Detuning measurements near the Cu L_3 edge after self-absorption correction (see Supplemental Material) [18]. (d) L dependence of CO correlation within the accessible range of [1.1, 1.8] r.l.u. at 930 eV, collected with σ polarization.

CO peaks identified in $YBa_2Cu_3O_{7-x}$ [11,20], albeit with a weaker intensity (see Supplemental Material) [18]. Thus, we will refer to this feature as the CO correlation below. Notably, here the CO wave vector $q_{CO} = (0.165, 0)$ is much smaller than that at underdoped LSCO samples—typically $q_{CO} \sim (0.23, 0)$ [16,34,35]. It nevertheless is close to the value in overdoped Bi2201 with $q_{CO} \sim (0.13, 0)$ [17], suggesting that charge instability with relatively long wavelength may prevail in heavily overdoped cuprates.

To investigate whether this CO correlation originates from CuO_2 planes, we also perform Cu L-edge resonant energy-integrated x-ray scattering (REIXS) measurements at UE46 PGM-1, Helmholtz-Zentrum Berlin. As shown in Fig. 2(a), we have measured the CO peak along $(0, -K)$ direction [blue cut in Fig. 1(e)] at both Cu L edge and O K edge and found it identical at the two edges, suggesting the strong hybridization between the Cu $3d$ and the O $2p$ orbitals. We revealed the presence of CO correlation along both H and K directions, which could arise either from a one-dimensional charge stripe along a^* or b^* direction with two domains or from a two-dimensional checkerboard pattern. Our results do not distinguish between these two scenarios and forthcoming measurements will be necessary to address this issue. We again observe that the CO peak is stronger at σ polarization than π polarization at Cu L edge [Fig. 2(b)] in favor of a charge origin [10]. Moreover, the peak measured by REIXS overlaps very well with the energy-integrated RIXS result (see Supplemental Material, Fig. S7) [18], proving the consistency of the two experimental techniques. Figure 2(c) shows the incident energy dependence of CO peak across Cu L_3 edge, which does not display a clear resonant behavior due to a relatively poor energy resolution of ~1.3 eV of REIXS measurement. By selecting the incident x-ray energy at 930 eV with a prominent CO peak, we further investigate the L dependence of CO [Fig. 2(d)]. We observe that the CO peak maximizes at $L = 1.1$ r.l.u. with smaller L value inaccessible, which is close to an integer L value. This is in sharp contrast to the behavior of CO in underdoped LSCO [35], which has a maximum at half-integer L due to the modulation of stripes along the c direction [36]. The different L behaviors may relate to the disappearance of spin glass phase beyond the critical doping of the pseudogap phase ($x_c \sim 0.19$) in LSCO [37], which is favored by charge-stripe ordering. It is worth noting that, in underdoped $YBa_2Cu_3O_{6+x}$, CO can be enhanced by suppressing superconductivity under a magnetic field [38,39], applying uniaxial strain [40], or through optical pump excitation [41]. Interestingly, these studies also reveal a peak at integer L values. Additionally, it is noteworthy that epitaxially grown $YBa_2Cu_3O_{6+x}$ thin films exhibit integer L CO up to room temperature, which may be favored by enhanced Fermi surface nesting conditions [42]. The similar L-dependent behaviors of CO induced by external controls and observed in the metallic region suggest common interlayer correlations and suggest that CO is a prevalent feature in the normal state.

To unveil the origin of CO, it is crucial to investigate its collective excitations and the interplay between CO and phonons. In underdoped cuprates, it is widely observed that CO coexists with phonon intensity anomaly near the characteristic wave vector, accompanied by different magnitudes of phonon energy softening [16,21,31,32,34,43]. These have been explained either by enhanced electron-phonon coupling [34] or interference between collective charge fluctuations and phonons [31,32,43]. Exploiting the high-energy resolution of O K edge RIXS, we can probe CO correlation and low-energy excitations at the same time. The RIXS map with better resolution (~25 meV) are visualized in Fig. 3(a) and Fig. 3(b). Notably, two phonon branches display pronounced enhancements of intensity near q_{CO}, while the phonon energy softening is negligible here. To quantify the $q_{||}$ dependence of the phonons, we fit the inelastic part of RIXS spectra and reveal three features at ~14, ~45, and ~75 meV (see Supplemental Material, Fig. S6) [18]. They can be assigned

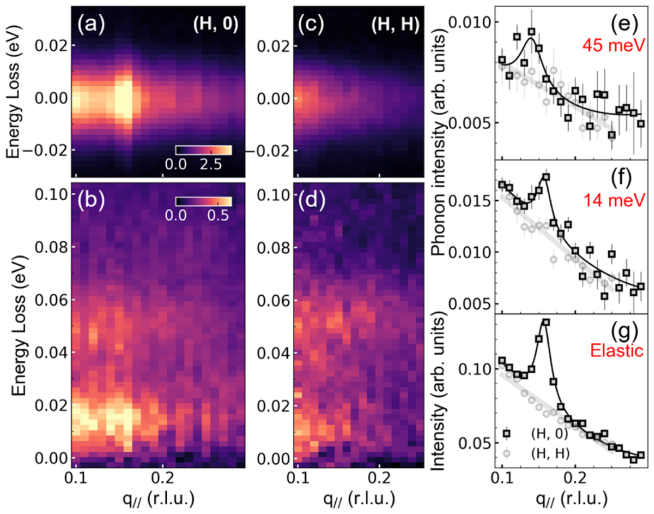

FIG. 3. Anisotropic momentum dependence of phonon intensity and dispersive CO excitations in $La_{2-x}Sr_xCuO_4$ ($x = 0.45$). (a),(c) The elastic intensity map and (b),(d) the inelastic RIXS intensity map for visualizing the CO correlation and phonon branches along $(H, 0)$ direction and (H, H) direction, respectively. (e)–(g) Integrated intensity for buckling phonon, acoustic phonon, and CO correlation, respectively, along both directions. Details of the fitting are presented in the Supplemental Material [18].

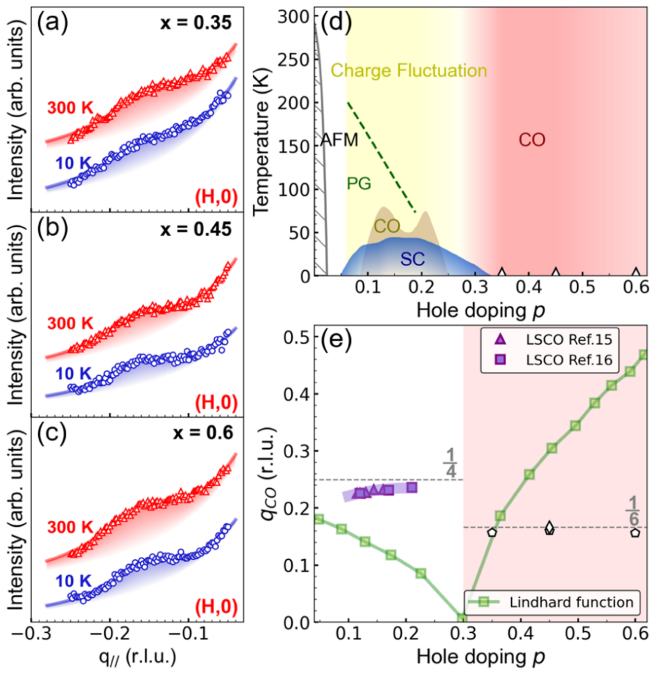

FIG. 4. Doping dependence of charge order correlation in overdoped $La_{2-x}Sr_xCuO_4$ (LSCO) and the extended phase diagram. (a)–(c) CO peak profiles measured by Cu L edge REIXS in LSCO with $x = 0.35, 0.45, 0.6$, respectively. The offset is applied for clarity. L is fixed at 1.1 r.l.u. The peak is nearly temperature independent up to 300 K. (d) The extended CO phase diagram of cuprates. It shows superconducting dome defined by T_c, antiferromagnetism (AFM) defined by T_N [44], pseudogap determined from the Nernst coefficient [45], underdoped charge order and charge fluctuation [16,35,46], and overdoped charge order. (e) The doping dependence of the CO wave vector in LSCO and nesting vector obtained from Lindhard function.

to the acoustic, bond-buckling, and bond-stretching phonon modes, respectively, in accord with a recent RIXS study on the optimally doped LSCO [21]. Our intensity distribution curves show that acoustic [Fig. 3(e)] and buckling [Fig. 3(f)] branches are reinforced near q_{CO} [Fig. 3(g)], in concert with a proposed picture that dynamical CO excitations interfere with multiple phonon branches [31,32,43]. In stark contrast, no phonon intensity anomalies have been observed along (H, H) direction in the absence of CO peak [Figs. 3(c) and 3(d)], which suggests an intimate correlation between phonon and CO correlation. We can further estimate the characteristic velocity of the dispersive CO excitations by connecting the maximal intensity anomaly of buckling mode at $q_A = 0.14$ r.l.u. with $q_{CO} = 0.16$ r.l.u., giving a velocity of $\sim 1.4 \pm 0.4$ eV Å. This matches very well with the CO velocity of 1.3 ± 0.3 eV Å in underdoped Bi2201 [32]. Our results indicate that dispersive CO excitations also exist in extremely overdoped regions, in analogy to those in underdoped regions.

To investigate the generality of this CO correlation, we study the doping dependence on another batch of overdoped LSCO thin films ($x = 0.35, 0.45, 0.6$) (Fig. 4). These films have a smaller thickness of 30 unit cells than the above-studied LSCO ($x = 0.45$) with 50 unit cells. We observe that the CO appears at $x = 0.35$ and gets more pronounced at $x = 0.45$ and 0.6, which all persist from 10 up to 300 K, as shown in Figs. 4(a)–4(c). We fit the REIXS spectrum with a Lorentz function for the peak and a Lorentz background from the specular tail, and the extracted peaks are shown in shaded areas. With smaller thickness, we observe that the CO peak displays a similar wave vector at ~0.166 r.l.u., but its correlation length becomes much shorter (~3 lattice units). The underlying cause of this thickness dependence remains to be fully understood. Our XRD measurements reveal similar lattice parameters of LSCO thin films as single crystals, ruling out the possibility of strain-induced CO (see Supplemental Material, Table I) [18]. Additionally, angle-resolved photoemission spectroscopy studies on LSCO thin films [47] demonstrate similar electronic structures as single crystals [22]. This suggests that the reentrant CO is a universal feature of LSCO, not limited to thin films.

The observation of CO correlation in extremely overdoped cuprates provides fresh insight for understanding the phase diagram [Fig. 4(d)]. The presence of CO and AFM phases on the two sides of the superconducting dome is enlightening, suggesting that the unconventional superconductivity of cuprates can be regarded as an emergent phase out of either AFM or CO. This is consistent with the

coexistence of short-ranged spin and charge fluctuations in the superconducting regime. Previous x-ray scattering studies on LSCO have revealed the CO peak at half-integer L values that disappears at $x \sim 0.25$ [16,35]. Recent research has shown that LSCO exhibits long-range temperature-dependent CO for $x < 0.15$ and short-range temperature-independent correlation for $0.15 < x \leq 0.2$ [48]. The reentrant CO in heavily overdoped LSCO behaves like the short-range correlation in LSCO [48] and the charge density fluctuation (CDF) in (Y,Nd)$Ba_2Cu_3O_{7-x}$ [46], indicating dynamic CO behavior. However, the CO correlation length in LSCO ($x = 0.45$) can be approximately 5 times longer than that of CDF ($\sim 4a$) [46]. Thus, it remains uncertain whether the observed CO correlation is fluctuating or not. Intriguingly, a similar behavior has been observed in infinite-layer $NdNiO_2$ nickelates, where the CO undergoes a transition to temperature-independent dynamical CO fluctuations above 100 K, exhibiting a correlation length of up to 60 Å [49]. The unique L dependence and in-plane wave vectors of the reentrant CO imply that different interactions are involved compared to CO in the underdoped region.

We then discuss the possible origins of this reentrant overdoped CO correlation. First, its emergence at the extremely overdoped region implies that it does not correlate with the pseudogap phase that ends at $x_c \sim 0.19$ [45]. We can also exclude the impact of the Van Hove singularity, which was argued to cause the charge density wave phase in Bi2201 [17], since the Lifshitz transition occurs at much lower doping for LSCO ($x \sim 0.2$) [35]. Figure 4(e) shows the doping dependence of q_{CO} in LSCO [15,16]. In the underdoped region, the CO wave vector increases with doping but close to 0.25 r.l.u. due to the proximity of spin and charge instabilities [50], while at the overdoped region it is likely to pin to a commensurate vector of $q_{CO} \sim 0.166$ r.l.u. The Fermi-surface (FS) instabilities induced by the Coulomb interactions may lead to charge fluctuations in the sense of perturbation theory [51]. Accordingly, we have calculated the Lindhard function for LSCO and tracked the doping dependence of the FS nesting vector along the $(H, 0)$ direction. The nesting vector shows a nonmonotonic behavior with a dip at $p \sim 0.3$ due to the Lifshitz transition from holelike FS to electronlike FS (see Supplemental Material, Fig. S8) [18]. This cannot account for the nearly doping-independent wave vector at $(0.166, 0)$, suggesting that the FS instability is an unlikely route to explain the CO correlation in the overdoped regime.

Our discovery of charge order correlation in heavily overdoped cuprates highlights the prevalence of electronic phase segregation in correlated electron systems and suggests that the highly overdoped regime harbors unexplored and interesting physics that requires a novel theoretical perspective. Recent research has shown that superconductivity can even occur in highly overdoped $La_{2-x}Ca_xCuO_4$ thin films with doping levels up to $x = 0.5$ [52], which raises the possibility of future experiments that explore the relationship between superconductivity and charge order in the extremely overdoped regime. A better understanding of this regime could shed light on other important properties of the cuprate phase diagram and inspire further experimental studies. Our findings that superconductivity emerges in the vicinity of the charge order phase share similarities with those of layered dichalcogenides Cu_xTiSe_2 [53] and infinite-layer nickelates [54], suggesting CO correlations may play a similar role to superconductivity in broad classes of superconductors. This presents new avenues for exploring the competition between charge order states and superconductivity in a wide range of correlated electron systems.

We thank M. Grill, E. Huang, H. Yao, J. Zhang, X. J. Zhou, Y. Li, F. Wang, N. L. Wang, J. Feng, and Z. Y. Weng for enlightening discussions. Y. P. acknowledges the financial support from the Ministry of Science and Technology of China (Grants No. 2019YFA0308401 and No. 2021YFA1401903) and the National Natural Science Foundation of China (Grant No. 11974029). Y. X. acknowledges the financial support from the National Natural Science Foundation of China (Grant No. 12074334). I. E. and Y. W. acknowledge support from the National Science Foundation (NSF) Grant No. DMR-2038011. Y. W. also acknowledges support from NSF Grant No. DMR-2337930. The RIXS experimental data were collected at beamline 41A of the National Synchrotron Radiation Research Center (NSRRC) in Hsinchu 30076, Taiwan. The REIXS experimental data were collected at the UE46-PGM1 beamline of Bessy-II (Helmholtz-Zentrum Berlin, Germany). The simulation presented in this work used resources of the National Energy Research Scientific Computing Center, a DOE Office of Science User Facility supported by the Office of Science of the U.S. Department of Energy under Contract No. DE-AC02-05CH11231 using NERSC Award No. BES-ERCAP0023181.

*Q. L., H.-Y. H., and T. R. contributed equally to this work.
†yingying.peng@pku.edu.cn

[1] P. A. Lee, N. Nagaosa, and X.-G. Wen, Doping a Mott insulator: Physics of high-temperature superconductivity, Rev. Mod. Phys. **78**, 17 (2006).
[2] B. Keimer, S. A. Kivelson, M. R. Norman, S. Uchida, and J. Zaanen, From quantum matter to high-temperature superconductivity in copper oxides, Nature (London) **518**, 179 (2015).
[3] I. Božović, X. He, J. Wu, and A. Bollinger, Dependence of the critical temperature in overdoped copper oxides on superfluid density, Nature (London) **536**, 309 (2016).
[4] Y. He, S.-D. Chen, Z.-X. Li, D. Zhao, D. Song, Y. Yoshida, H. Eisaki, T. Wu, X.-H. Chen, D.-H. Lu *et al.*, Superconducting Fluctuations in Overdoped $Bi_2Sr_2CaCu_2O_{8+\delta}$, Phys. Rev. X **11**, 031068 (2021).
[5] M. P. M. Dean, G. Dellea, R. S. Springell, F. Yakhou-Harris, K. Kummer, N. B. Brookes, X. Liu, Y. J. Sun, J. Strle, T. Schmitt *et al.*, Persistence of magnetic excitations in

$La_{2-x}Sr_xCuO_4$ from the undoped insulator to the heavily overdoped non-superconducting metal, Nat. Mater. **12**, 1019 (2013).

[6] K. Kurashima, T. Adachi, K. M. Suzuki, Y. Fukunaga, T. Kawamata, T. Noji, H. Miyasaka, I. Watanabe, M. Miyazaki, A. Koda *et al.*, Development of Ferromagnetic Fluctuations in Heavily Overdoped $(Bi,Pb)_2Sr_2CuO_{6+\delta}$ Copper Oxides, Phys. Rev. Lett. **121**, 057002 (2018).

[7] J. Sonier, C. Kaiser, V. Pacradouni, S. Sabok-Sayr, C. Cochrane, D. MacLaughlin, S. Komiya, and N. Hussey, Direct search for a ferromagnetic phase in a heavily overdoped nonsuperconducting copper oxide, Proc. Natl. Acad. Sci. U.S.A. **107**, 17131 (2010).

[8] J. Tranquada, B. Sternlieb, J. Axe, Y. Nakamura, and S. Uchida, Evidence for stripe correlations of spins and holes in copper oxide superconductors, Nature (London) **375**, 561 (1995).

[9] P. Abbamonte, A. Rusydi, S. Smadici, G. Gu, G. Sawatzky, and D. Feng, Spatially modulated 'Mottness' in $La_{2-x}Ba_xCuO_4$, Nat. Phys. **1**, 155 (2005).

[10] G. Ghiringhelli, M. Le Tacon, M. Minola, S. Blanco-Canosa, C. Mazzoli, N. B. Brookes, G. M. De Luca, A. Frano, D. G. Hawthorn, F. He *et al.*, Long-range incommensurate charge fluctuations in $(Y,Nd)Ba_2Cu_3O_{6+x}$, Science **337**, 821 (2012).

[11] J. Chang, E. Blackburn, A. Holmes, N. B. Christensen, J. Larsen, J. Mesot, R. Liang, D. Bonn, W. Hardy, A. Watenphul *et al.*, Direct observation of competition between superconductivity and charge density wave order in $YBa_2Cu_3O_{6.67}$, Nat. Phys. **8**, 871 (2012).

[12] R. Comin, A. Frano, M. M. Yee, Y. Yoshida, H. Eisaki, E. Schierle, E. Weschke, R. Sutarto, F. He, A. Soumyanarayanan *et al.*, Charge order driven by Fermi-arc instability in $Bi_2Sr_{2-x}La_xCuO_{6+\delta}$, Science **343**, 390 (2014).

[13] Y. Y. Peng, M. Salluzzo, X. Sun, A. Ponti, D. Betto, A. M. Ferretti, F. Fumagalli, K. Kummer, M. Le Tacon, X. J. Zhou *et al.*, Direct observation of charge order in underdoped and optimally doped $Bi_2(Sr,La)_2CuO_{6+\delta}$ by resonant inelastic x-ray scattering, Phys. Rev. B **94**, 184511 (2016).

[14] P. Cai, W. Ruan, Y. Peng, C. Ye, X. Li, Z. Hao, X. Zhou, D.-H. Lee, and Y. Wang, Visualizing the evolution from the Mott insulator to a charge-ordered insulator in lightly doped cuprates, Nat. Phys. **12**, 1047 (2016).

[15] J.-J. Wen, H. Huang, S.-J. Lee, H. Jang, J. Knight, Y. S. Lee, M. Fujita, K. M. Suzuki, S. Asano, S. A. Kivelson *et al.*, Observation of two types of charge-density-wave orders in superconducting $La_{2-x}Sr_xCuO_4$, Nat. Commun. **10**, 3269 (2019).

[16] J. Q. Lin, H. Miao, D. G. Mazzone, G. D. Gu, A. Nag, A. C. Walters, M. García-Fernández, A. Barbour, J. Pelliciari, I. Jarrige *et al.*, Strongly Correlated Charge Density Wave in $La_{2-x}Sr_xCuO_4$ Evidenced by Doping-Dependent Phonon Anomaly, Phys. Rev. Lett. **124**, 207005 (2020).

[17] Y. Peng, R. Fumagalli, Y. Ding, M. Minola, S. Caprara, D. Betto, M. Bluschke, G. M. De Luca, and K. Kummer, Re-entrant charge order in overdoped $(Bi,Pb)_{2.12}Sr_{1.88}CuO_{6+\delta}$ outside the pseudogap regime, Nat. Mater. **17**, 697 (2018).

[18] See Supplemental Material at http://link.aps.org/supplemental/10.1103/PhysRevLett.131.116002 for sample preparation and characterization, details of RIXS and REIXS measurements, data fitting, and Lindhard analysis, which includes Refs. [17,19–29].

[19] A. Nag, M. Zhu, M. Bejas, J. Li, H. C. Robarts, H. Yamase, A. N. Petsch, D. Song, H. Eisaki, A. C. Walters *et al.*, Detection of Acoustic Plasmons in Hole-Doped Lanthanum and Bismuth Cuprate Superconductors Using Resonant Inelastic X-Ray Scattering, Phys. Rev. Lett. **125**, 257002 (2020).

[20] E. M. Forgan, E. Blackburn, A. T. Holmes, A. K. R. Briffa, J. Chang, L. Bouchenoire, S. D. Brown, R. Liang, D. Bonn, W. N. Hardy *et al.*, The microscopic structure of charge density waves in underdoped $YBa_2Cu_3O_{6.54}$ revealed by x-ray diffraction, Nat. Commun. **6**, 10064 (2015).

[21] H. Y. Huang, A. Singh, C. Y. Mou, S. Johnston, A. F. Kemper, J. van den Brink, P. J. Chen, T. K. Lee, J. Okamoto, Y. Y. Chu *et al.*, Quantum Fluctuations of Charge Order Induce Phonon Softening in a Superconducting Cuprate, Phys. Rev. X **11**, 041038 (2021).

[22] T. Yoshida, X. J. Zhou, K. Tanaka, W. L. Yang, Z. Hussain, Z.-X. Shen, A. Fujimori, S. Sahrakorpi, M. Lindroos, R. S. Markiewicz *et al.*, Systematic doping evolution of the underlying Fermi surface of $La_{2-x}Sr_xCuO_4$, Phys. Rev. B **74**, 224510 (2006).

[23] Q. Xiao, Y. Lin, Q. Li, X. Zheng, S. Francoual, C. Plueckthun, W. Xia, Q. Qiu, S. Zhang, Y. Guo *et al.*, Coexistence of multiple stacking charge density waves in kagome superconductor CsV_3Sb_5, Phys. Rev. Res. **5**, L012032 (2023).

[24] J. Chang, E. Blackburn, A. Holmes, N. B. Christensen, J. Larsen, J. Mesot, R. Liang, and D. A. Bonn, Direct observation of competition between superconductivity and charge density wave order in $YBa_2Cu_3O_{6.67}$, Nat. Phys. **8**, 871–876 (2012).

[25] H. Sato, A. Tsukada, M. Naito, and A. Matsuda, $La_{2-x}Sr_xCuO_y$ epitaxial thin films ($x = 0$ to 2): Structure, strain, and superconductivity, Phys. Rev. B **61**, 12447 (2000).

[26] G. Xu, Q. Pu, Z. Zhang, and Z. Ding, Phonon Vibration and Conduction of $La_{2-x}Sr_xCuO_{4-\delta}$ and $La_{1.85-x}Sr_{0.15+x}Cu_{1-x}Co_xO_{4-\delta}$, J. Supercond. **15**, 141 (2002).

[27] N. B. Brookes, G. Ghiringhelli, A.-M. Charvet, A. Fujimori, T. Kakeshita, H. Eisaki, S. Uchida, and T. Mizokawa, Stability of the Zhang-Rice Singlet with Doping in Lanthanum Strontium Copper Oxide across the Superconducting Dome and above, Phys. Rev. Lett. **115**, 027002 (2015).

[28] A. Singh, H. Y. Huang, Y. Y. Chu, C. Y. Hua, S. W. Lin, H. S. Fung, H. W. Shiu, J. Chang, J. H. Li, J. Okamoto *et al.*, Development of the soft x-ray AGM–AGS RIXS beamline at the Taiwan photon source, J. Synchrotron Radiat. **28**, 977 (2021).

[29] A. Achkar, Inverse partial fluorescence yield spectroscopy, Master's thesis, University of Waterloo, 2011.

[30] C. T. Chen, F. Sette, Y. Ma, M. S. Hybertsen, E. B. Stechel, W. M. C. Foulkes, M. Schulter, S.-W. Cheong, A. S. Cooper, L. W. Rupp *et al.*, Electronic States in $La_{2-x}Sr_xCuO_{4+\delta}$ Probed by Soft-X-Ray Absorption, Phys. Rev. Lett. **66**, 104 (1991).

[31] L. Chaix, G. Ghiringhelli, Y. Peng, M. Hashimoto, B. Moritz, K. Kummer, N. B. Brookes, Y. He, S. Chen, S. Ishida *et al.*, Dispersive charge density wave excitations in $Bi_2Sr_2CaCu_2O_{8+\delta}$, Nat. Phys. **13**, 952 (2017).

[32] J. Li, A. Nag, J. Pelliciari, H. Robarts, A. Walters, M. Garcia-Fernandez, H. Eisaki, D. Song, H. Ding, S. Johnston *et al.*, Multiorbital charge-density wave excitations and concomitant phonon anomalies in $Bi_2Sr_2LaCuO_{6+\delta}$, Proc. Natl. Acad. Sci. U.S.A. **117**, 16219 (2020).

[33] A. J. Achkar, F. He, R. Sutarto, C. McMahon, M. Zwiebler, M. Hücker, G. D. Gu, R. Liang, D. A. Bonn, W. N. Hardy *et al.*, Orbital symmetry of charge-density-wave order in $La_{1.875}Ba_{0.125}CuO_4$ and $YBa_2Cu_3O_{6.54}$, Nat. Mater. **15**, 616 (2016).

[34] Y. Y. Peng, A. A. Husain, M. Mitrano, S. X.-L. Sun, T. A. Johnson, A. V. Zakrzewski, G. J. MacDougall, A. Barbour, I. Jarrige, V. Bisogni *et al.*, Enhanced Electron-Phonon Coupling for Charge-Density-Wave Formation in $La_{1.8-x}Eu_{0.2}Sr_xCuO_{4+\delta}$, Phys. Rev. Lett. **125**, 097002 (2020).

[35] H. Miao, G. Fabbris, R. Koch, D. G. Mazzone, C. S. Nelson, R. Acevedo-Esteves, G. D. Gu, Y. Li, T. Yilimaz, K. Kaznatcheev *et al.*, Charge density waves in cuprate superconductors beyond the critical doping, npj Quantum Mater. **6**, 31 (2021).

[36] H. Kimura, H. Goka, M. Fujita, Y. Noda, K. Yamada, and N. Ikeda, Synchrotron x-ray diffraction study of a charge stripe order in $\frac{1}{8}$-doped $La_{1.875}Ba_{0.125-x}Sr_xCuO_4$, Phys. Rev. B **67**, 140503(R) (2003).

[37] M. Frachet, I. Vinograd, R. Zhou, S. Benhabib, S. Wu, H. Mayaffre, S. Krämer, S. K. Ramakrishna, A. P. Reyes, J. Debray *et al.*, Hidden magnetism at the pseudogap critical point of a cuprate superconductor, Nat. Phys. **16**, 1064 (2020).

[38] S. Gerber, H. Jang, H. Nojiri, S. Matsuzawa, H. Yasumura, D. A. Bonn, R. Liang, W. N. Hardy, Z. Islam, A. Mehta *et al.*, Three-dimensional charge density wave order in $YBa_2Cu_3O_{6.67}$ at high magnetic fields, Science **350**, 949 (2015).

[39] T. Wu, H. Mayaffre, S. Krämer, M. Horvatić, C. Berthier, W. N. Hardy, R. Liang, D. A. Bonn, and M.-H. Julien, Magnetic-field-induced charge-stripe order in the high-temperature superconductor $YBa_2Cu_3O_y$, Nature (London) **477**, 191 (2011).

[40] H.-H. Kim, S. M. Souliou, M. E. Barber, E. Lefrançois, M. Minola, M. Tortora, R. Heid, N. Nandi, R. A. Borzi, G. Garbarino *et al.*, Uniaxial pressure control of competing orders in a high-temperature superconductor, Science **362**, 1040 (2018).

[41] H. Jang, S. Song, T. Kihara, Y. Liu, S.-J. Lee, S.-Y. Park, M. Kim, H.-D. Kim, G. Coslovich, S. Nakata *et al.*, Characterization of photoinduced normal state through charge density wave in superconducting $YBa_2Cu_3O_{6.67}$, Sci. Adv. **8**, eabk0832 (2022).

[42] M. Bluschke, A. Frano, E. Schierle, D. Putzky, F. Ghorbani, R. Ortiz, H. Suzuki, G. Christiani, G. Logvenov, E. Weschke *et al.*, Stabilization of three-dimensional charge order in $YBa_2Cu_3O_{6+x}$ via epitaxial growth, Nat. Commun. **9**, 2978 (2018).

[43] W. S. Lee, K.-J. J. Zhou, M. Hepting, J. Li, A. Nag, A. C. Walters, M. Garcia-Fernandez, H. C. Robarts, M. Hashimoto, H. Lu *et al.*, Spectroscopic fingerprint of charge order melting driven by quantum fluctuations in a cuprate, Nat. Phys. **17**, 53 (2021).

[44] K. Yamada, C. H. Lee, K. Kurahashi, J. Wada, S. Wakimoto, S. Ueki, H. Kimura, Y. Endoh, S. Hosoya, G. Shirane *et al.*, Doping dependence of the spatially modulated dynamical spin correlations and the superconducting-transition temperature in $La_{2-x}Sr_xCuO_4$, Phys. Rev. B **57**, 6165 (1998).

[45] Y. Wang, L. Li, and N. P. Ong, Nernst effect in high-T_c superconductors, Phys. Rev. B **73**, 024510 (2006).

[46] R. Arpaia, S. Caprara, R. Fumagalli, G. D. Vecchi, Y. Y. Peng, E. Andersson, D. Betto, G. M. D. Luca, N. B. Brookes, F. Lombardi *et al.*, Dynamical charge density fluctuations pervading the phase diagram of a Cu-based high T_c superconductor, Science **365**, 906 (2019).

[47] Y. Zhong, Z. Chen, S.-D. Chen, K.-J. Xu, M. Hashimoto, Y. He, S. ichi Uchida, D. Lu, S.-K. Mo, and Z.-X. Shen, Differentiated roles of Lifshitz transition on thermodynamics and superconductivity in $La_{2-x}Sr_xCuO_4$, Proc. Natl. Acad. Sci. U.S.A. **119**, e2204630119 (2022).

[48] K. von Arx, Q. Wang, S. Mustafi, D. G. Mazzone, M. Horio, D. J. Mukkattukavil, E. Pomjakushina, S. Pyon, T. Takayama, H. Takagi *et al.*, Fate of charge order in overdoped La-based cuprates, npj Quantum Mater. **8**, 7 (2023).

[49] C. C. Tam, J. Choi, X. Ding, S. Agrestini, A. Nag, M. Wu, B. Huang, H. Luo, P. Gao, M. García-Fernández *et al.*, Charge density waves in infinite-layer $NdNiO_2$ nickelates, Nat. Mater. **21**, 1116 (2022).

[50] L. Nie, A. V. Maharaj, E. Fradkin, and S. A. Kivelson, Vestigial nematicity from spin and/or charge order in the cuprates, Phys. Rev. B **96**, 085142 (2017).

[51] E. G. Dalla Torre, D. Benjamin, Y. He, D. Dentelski, and E. Demler, Friedel oscillations as a probe of fermionic quasiparticles, Phys. Rev. B **93**, 205117 (2016).

[52] G. Kim, K. S. Rabinovich, A. V. Boris, A. N. Yaresko, Y. E. Suyolcu, Y.-M. Wu, P. A. van Aken, G. Christiani, G. Logvenov, and B. Keimer, Optical conductivity and superconductivity in highly overdoped $La_{2-x}Ca_xCuO_4$ thin films, Proc. Natl. Acad. Sci. U.S.A. **118**, e2106170118 (2021).

[53] Y. I. Joe, X. M. Chen, P. Ghaemi, K. D. Finkelstein, G. A. de la Peña, Y. Gan, J. C. T. Lee, S. Yuan, J. Geck, G. J. MacDougall *et al.*, Emergence of charge density wave domain walls above the superconducting dome in 1T-$TiSe_2$, Nat. Phys. **10**, 421 (2014).

[54] M. Rossi, M. Osada, J. Choi, S. Agrestini, D. Jost, Y. Lee, H. Lu, B. Y. Wang, K. Lee, A. Nag *et al.*, A broken translational symmetry state in an infinite-layer nickelate, Nat. Phys. **18**, 869 (2022).